were corrected for twofold dilution upon Alexa-PBD addition. Alexa-PBD concentrations were either varied as shown, or maintained at 1 micromolar when saturating Alexa-PBD was required. The spectra shown were corrected for direct excitation of the Alexa fluorophore by acquiring spectra of Alexa-PBD alone at equivalent concentrations, and subtracting these from spectra shown in Fig. 2. Values for K_d were determined by fitting to the equation: $Y = A*X/(K_d + X)$. Higher, saturating concentrations of Alexa-PBD were not used because errors from subtraction of direct Alexa excitation became larger. The biological activity of GFP-Rac was previously verified (*5*). The GFP-Rac used for determination of equilibrium constants was shown to be >98% active in binding GTPγS, determined as described (*26*).

10. C. Chamberlain, data not shown.
11. E. Manser, T. Leung, H. Salihuddin, Z.-S. Zhao, L. Lim, *Nature* **367**, 40 (1994).
12. D. A. Leonard *et al.*, *Biochemistry* **36**, 1173 (1997).
13. G. Thompson, D. Owen, P. A. Chalk, P. N. Lowe, *Biochemistry* **37**, 7885 (1998).
14. L. Menard *et al.*, *Eur. J. Biochem.* **206**, 537 (1992).
15. A. J. Ridley, H. F. Paterson, C. L. Johnston, D. Diekmann, A. Hall, *Cell* **70**, 401 (1992).
16. P. T. Hawkins *et al.*, *Curr. Biol.* **5**, 393 (1995).
17. For serum stimulation experiments, Swiss 3T3 fibroblasts (ATCC, passage 15 through 27) were plated on glass coverslips and then maintained in Dulbecco's modified Eagle's medium (DMEM) with 10% fetal bovine serum (FBS), 1% L-glutamine, and 1% penicillin-streptomycin for at least 24 hours. Media was then replaced with media containing only 0.5% FBS, and cells were maintained for 42 hours. Cells were transfected by microinjecting 200 μg/ml pcDNA-EGFP-Rac plasmid into cell nuclei 2 to 8 hours before the experiment. The EGFP mutant was used in all experiments, cloned and expressed as described (*5*). Cells expressing the GFP-Rac were then microinjected with 100 mM Alexa-PBD. This concentration produced the appropriate levels of intracellular PBD (Fig. 2B) after the material was diluted when it entered the cells. Cells were mounted in a heated chamber on a Zeiss Axiovert 100TV microscope and maintained in Dulbecco's phosphate-buffered saline (DPBS) (Gibco) to reduce background fluorescence. Cells were then stimulated by replacing the media with DPBS containing 10% FBS or 50 ng/mL PDGF. Images were obtained every 30 s using a Photometrics PXL-cooled CCD camera with 1 × 1 or 3 × 3 binning, and a Zeiss 40× 1.3 NA oil-immersion objective. Fluorescence filters from Chroma were as follows: GFP: HQ480/40, HQ535/50, Q505LP; FRET: D480/30, HQ610/75, 505LP; Alexa: HQ 545/30, HQ 610/75, Q565LP. Cells were illuminated using a 100-W Hg arc lamp. Exposure times for 3 × 3 binning were: GFP, 0.1 s; Alexa-PBD, 0.1 s; and FRET, 0.5 s. For 1 × 1 binning, exposure times were: GFP, 1 s; Alexa-PBD, 1 s, and FRET, 5 s.
18. Images were first background-subtracted and registered to ensure accurate pixel alignment. The GFP-Rac image was then thresholded, changing the intensities of all pixels outside of the cell to zero. Thresholding was based on the GFP image because it had the largest signal-to-noise ratio, providing the clearest distinction between the cell and background. The thresholded GFP-Rac image was used to generate a binary image with all values within the cell = 1 and all outside = 0. The FRET and Alexa-PBD images were multiplied by the binary image, ensuring that the same pixels were analyzed in all three images. Emission appearing in the FRET image from direct excitation of Alexa and GFP was removed by subtracting a fraction of the GFP-Rac and Alexa-PBD images from the FRET image. This fraction depended on the filter set and exposure conditions used. It was determined, as described in detail elsewhere (*27*), by taking images of cells containing only GFP-Rac or Alexa-PBD alone, and quantifying the relative intensity of emission in the FRET channel and that in the GFP or Alexa-PBD channel. A broad range of intensities was examined and a line was fit to these for accurate determinations. These corrections had to be applied carefully when studying rapidly moving objects such as ruffles. If the ruffle moved between acquisition of the FRET, GFP, or Alexa images, the subtractive correction process would remove light from the FRET image in the wrong place, generating artifactual FRET localizations. Data from moving features were used only when careful inspection showed the feature to be coincident in the Alexa, GFP, and FRET images, and controls were performed with images taken in different orders. A low-pass filter kernel was applied to the corrected FRET image to remove high-frequency noise (*28*). Image processing and microscope automation were performed using Inovision ISEE software. Images were contrast stretched and formated for display using Adobe Photoshop software. We tested Rac and PBD fused to GFP mutants that undergo FRET (ECFP and EYFP). Unfortunately, their spectral overlap was more problematic than that of Alexa and GFP, making the corrections described here more difficult. In addition, the GFP mutants showed roughly 25% the FRET of FLAIR. We used FLAIR for these reasons, but the ability to monitor Rac activity simply through protein expression may justify using GFP mutants in some applications.
19. C. Y. Chung, S. Lee, C. Briscoe, C. Ellsworth, R. A. Firtel, *Proc. Natl. Acad. Sci. U.S.A.* **97**, 5225 (2000).
20. For wound-healing experiments, Swiss 3T3 fibroblasts were induced to undergo polarized movement as described (*29*). The cells were cultured in Dulbecco's modified Eagle's medium (Gibco) supplemented with 10% FBS at 37°C. Cells were trypsinized and then plated on glass coverslips. They were grown to a confluent monolayer and maintained for an additional 3 to 4 days. Cells were then wounded by creating a straight laceration with a sterile razor blade. Cells along the edge of the wound were microinjected with 200 μg/ml pcDNA-EGFP-Rac plasmid DNA. Six hours after the wound was formed, cells expressing the GFP-Rac were microinjected with 100 micromolar Alexa-PBD and allowed ~10 min for recovery. Media was then replaced with DPBS containing 10% FBS to reduce background fluorescence. Images were obtained as described above, using exposure times of 1 s for GFP, 1 s for Alexa-PBD, and 5 s for FRET.
21. Y. L. Wang, *J. Cell Biol.* **101**, 597 (1985).
22. J. A. Theriot and T. J. Mitchison, *Nature* **352**, 126 (1991).
23. F. Michiels *et al.*, *Nature* **375**, 338 (1995).
24. T. Joneson, *Mol. Cell. Biol.* **19**, 5892 (1999).
25. R. Y. Tsien, *Annu. Rev. Biochem.* **67**, 509 (1998).
26. U. G. Knaus, P. G. Heyworth, B. T. Kinsella, J. T. Curnutte, G. M. Bokoch, *J. Biol. Chem.* **267**, 23575 (1992).
27. C. E. Chamberlain, V. Kraynov, K. M. Hahn, *Methods Enzymol.*, in press.
28. K. Castleman, *Digital Image Processing* (Prentice-Hall, Upper Saddle River, NJ, 1996), pp. 207–209.
29. R. DeBiasio, G. R. Bright, L. A. Ernst, A. S. Waggoner, D. L. Taylor, *J. Cell Biol.* **105**, 1613 (1987).
30. J. R. Lakowicz, *Principles of Fluorescence Spectroscopy* (Plenum, New York, 1983), pp. 305–341.

31. The thoughtful comments of M. Symons and C. Waterman-Storer are much appreciated. We thank R. Tsien for providing the EGFP mutant, P. Millman of Chroma for help with filter design, D. Benson and M. Sims of Inovision for help in image analysis and microscope automation, V. Benard for assistance with preparation of PBD, S. Junger for technical assistance, and E. Blanc for expert administrative assistance. For their financial support, we thank NIH (grants R01 GM-57464 and AG15430 to K.M.H. and GM39434 and GM44428 to G.M.B.) and the Arthritis Foundation for a postdoctoral fellowship to V.S.K.

5 June 2000; accepted 25 August 2000

A Myosin I Isoform in the Nucleus

Lidija Pestic-Dragovich,[1]* Ljuba Stojiljkovic,[1]* Anatoly A. Philimonenko,[2] Grzegorz Nowak,[1] Yunbo Ke,[1] Robert E. Settlage,[3] Jeffrey Shabanowitz,[3] Donald F. Hunt,[4] Pavel Hozak,[2] Primal de Lanerolle[1]†

A nuclear isoform of myosin I β that contains a unique 16–amino acid amino-terminal extension has been identified. An affinity-purified antibody to the 16–amino acid peptide demonstrated nuclear staining. Confocal and electron microscopy revealed that nuclear myosin I β colocalized with RNA polymerase II in an α-amanitin– and actinomycin D–sensitive manner. The antibody coimmunoprecipitated RNA polymerase II and blocked in vitro RNA synthesis. This isoform of myosin I β appears to be in a complex with RNA polymerase II and may affect transcription.

Myosin I is a single-headed, nonfilamentous member of the myosin superfamily of actin-based molecular motors (*1, 2*). There are at least four different subclasses of myosin I proteins, all containing a 110- to 150-kD heavy chain and one to six light chains. Myosin I is diffusely distributed throughout the cytoplasm (*3*). It concentrates near cortical surfaces and in the perinuclear region (*3*), and it appears to mediate plasma membrane extension (*3, 4*), vesicle and organelle transport (*5*), and mechanochemical regulation of calcium channels in hair cells (*6*).

Affinity-purified polyclonal antibodies to bovine adrenal myosin I recognized a 120-kD protein that is larger than the antigen (116 kD) (*7*). Confocal and electron microscopy showed cytoplasmic and nuclear staining with these antibodies. Biochemical assays on nuclei demonstrated that the 120-kD protein binds adenosine triphosphate (ATP) and calmodulin, is associated with K^+-EDTA ATPase activity, and

[1]Department of Physiology and Biophysics, University of Illinois at Chicago, Chicago, IL 60612, USA. [2]Department of Cell Ultrastructure and Molecular Biology, Institute of Experimental Medicine, Academy of Sciences of the Czech Republic, Prague, Czech Republic. [3]Chemistry Department, University of Virginia, Charlottesville, VA 22901, USA. [4]Departments of Chemistry and Pathology, University of Virginia, Charlottesville, VA 22901, USA.

*These authors contributed equally to this paper.
†To whom correspondence should be addressed. E-mail: primal@uic.edu

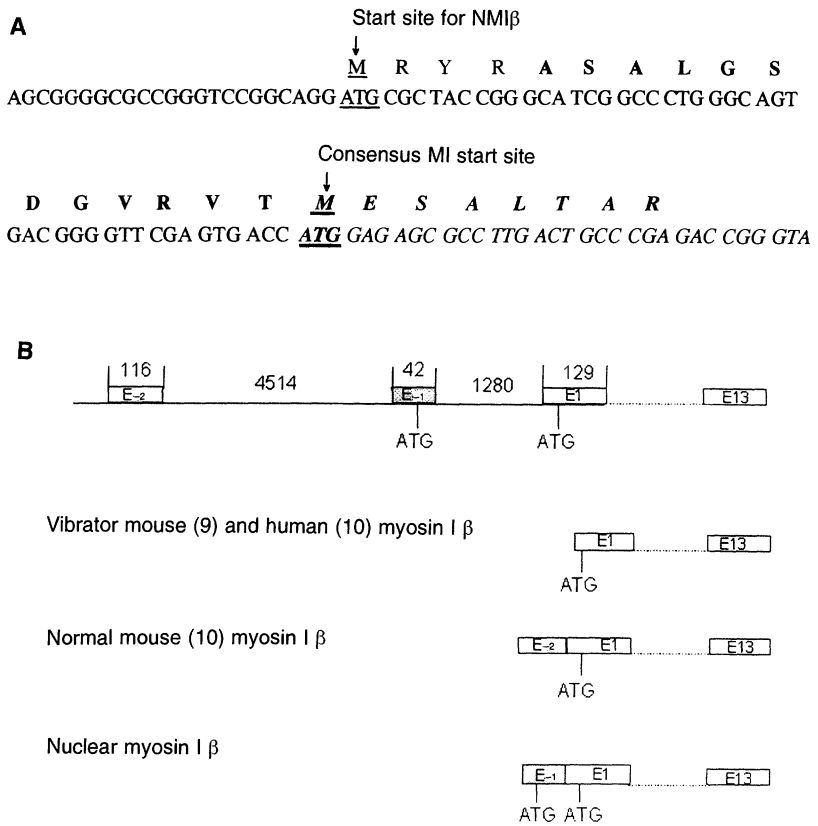

Fig. 1. Structure of the myosin I β gene (*29*). (**A**) The ATG's corresponding to NMIβ and consensus start sites are underlined. The peptide obtained by microsequencing that overlaps the consensus start site is shown in bold. The known mouse myosin I β cDNA and protein sequences (*9, 10*) are in italics. PCR amplification and DNA sequencing of the NMIβ cDNA showed that the coding region is identical to other mouse myosin I β coding sequences (*9, 10*) and nearly identical (>98% homology) to the rat myosin I β coding sequence (*11*). (**B**) The structure of the myosin I β gene in the mouse, rat, and human. The myosin I β gene is in an 80-kb region of chromosome 11 (*13*) that may contain a mutation that causes a serious neurological and behavioral disorder in the vibrator mouse (*9*). At least two mRNA species that code for myosin I β in vibrator and normal mice, with identical protein coding regions but different 5′UTRs, have also been reported (*9, 10*). NMIβ starts with the ATG in exon −1. The NMIβ cDNA is similar to a cDNA (myr 2) that contains two potential start sites and codes for a single, cytoplasmic protein in adult rats (*11*). The GenBank accession number for the nucleotide sequence is AY007255.

Table 1. A statistical analysis performed on three independent double-labeling immunoelectron microscopy colocalization experiments (Fig. 4) (*21*) demonstrated statistically significant numbers of NMIβ and RNA Pol II within 100 nm of each other in control cells. This distribution was disrupted and the colocalization of NMIβ and RNA Pol II was insignificant at <100 nm after inhibition of RNA transcription. NS, not significant ($P > 0.05$).

Treatment	Density of RNA Pol II label (5-nm particles/μm²)	Density of NMIβ label (10-nm particles/μm²)	Statistical significance		
			0 to 30 nm	30 to 100 nm	100 to 200 nm
None (control)	32.46	8.34	$P < 0.05$	$P < 0.01$	$P < 0.01$
α-Amanitin	9.52	10.87	NS	NS	$P < 0.01$
Actinomycin D	25.31	10.51	NS	NS	$P < 0.01$

binds actin only in the absence of ATP (*7*). Because these characteristics are defining features of the myosin superfamily of proteins (*1*), we considered the possibility that the 120-kD protein is a myosin I isoform that is a nuclear molecular motor.

The 120-kD protein was immunoprecipitated from nuclei isolated from mouse fibroblasts (*8*). SDS–polyacrylamide gel electrophoresis (PAGE) showed a 120-kD band by Coomassie blue staining in the immunoprecipitates. Microsequencing of the 120-kD protein (*8*) revealed high sequence homology (>98%) with myosin I β. It also revealed the presence of 12 amino acids preceding the consensus initiator methionine (*9–11*) of myosin I β.

Analysis of an embryonic mouse cDNA library with mouse myosin I β primers (*12*) yielded two sequences. The shorter of the two sequences encoded a peptide that contained the consensus mouse myosin I β start site (*9, 10*). The longer sequence contained another upstream start site that is followed by nucleotides that encode a 16–amino acid sequence (Fig. 1A) that is not found in other myosin I β proteins (*1–6, 9–11*). Moreover, 12 of the 16 amino acids exactly matched the 12 amino acids that were found by microsequencing the 120-kD protein. Therefore, the 120-kD protein (119,720 daltons, as calculated from the amino acid sequence) is referred to as nuclear myosin I β (NMIβ) to differentiate it from the smaller (117,999 daltons), exclusively cytoplasmic myosin I β isoform (CMIβ).

The mouse myosin I β gene is located on chromosome 11 (*9, 13*). It contains 13 exons, starting with exon 1, and is ~12 kb long. Two additional exons (exons −2 and −1) were located upstream of exon 1 on chromosome 11 (Fig. 1B). Exon −2 is found in the 5′ untranslated region (5′UTR) of the normal adult mouse myosin I β cDNA (*10*). Exon −1 is not found in other mouse myosin I β cDNAs (*9, 10*). Exon −1 contains a second translation start site that is in frame with the consensus myosin I β translation start site on exon 1. Translation starting from the ATG on exon −1, which is preceded by a Kozak sequence (*14*), produces a protein identical to mouse myosin I β but with 16 additional amino acids at the NH_2-terminus. The first six amino acids come from exon −1 and the remaining 10 amino acids come from exon 1. Exon −1 also contributes 24 nucleotides, very rich in GC, that constitute the 5′UTR of NMIβ. Thus, the NMIβ and CMIβ isoforms appear to be translated from separate transcripts originating from the same gene on chromosome 11.

To determine whether the 16–amino acid extension directs NMIβ to the nucleus, we cloned the cDNA for the NMIβ and CMIβ isoforms into a vector containing the FLAG epitope and transfected the result into NIH 3T3 cells (*15*). Confocal microscopy showed that CMIβ-FLAG was confined to the cytoplasm (Fig. 2, A to D). In contrast, there was nuclear and cytoplasmic expression of the NMIβ-FLAG (Fig. 2, E to H). Experiments were also performed with an affinity-purified antibody to the 16–amino acid peptide (*16*). This antibody recognized a 120-kD protein by protein immunoblotting (Fig. 3) and also stained the nucleus (Fig. 2, I to L). There was no staining when the affinity-purified antibody to NMIβ peptide was adsorbed with the peptide before staining (Fig. 2, M to P). These data suggest that the unique, 16–amino acid NH_2-terminal extension directs NMIβ to the nucleus.

Confocal microscopy (*17*) also showed that

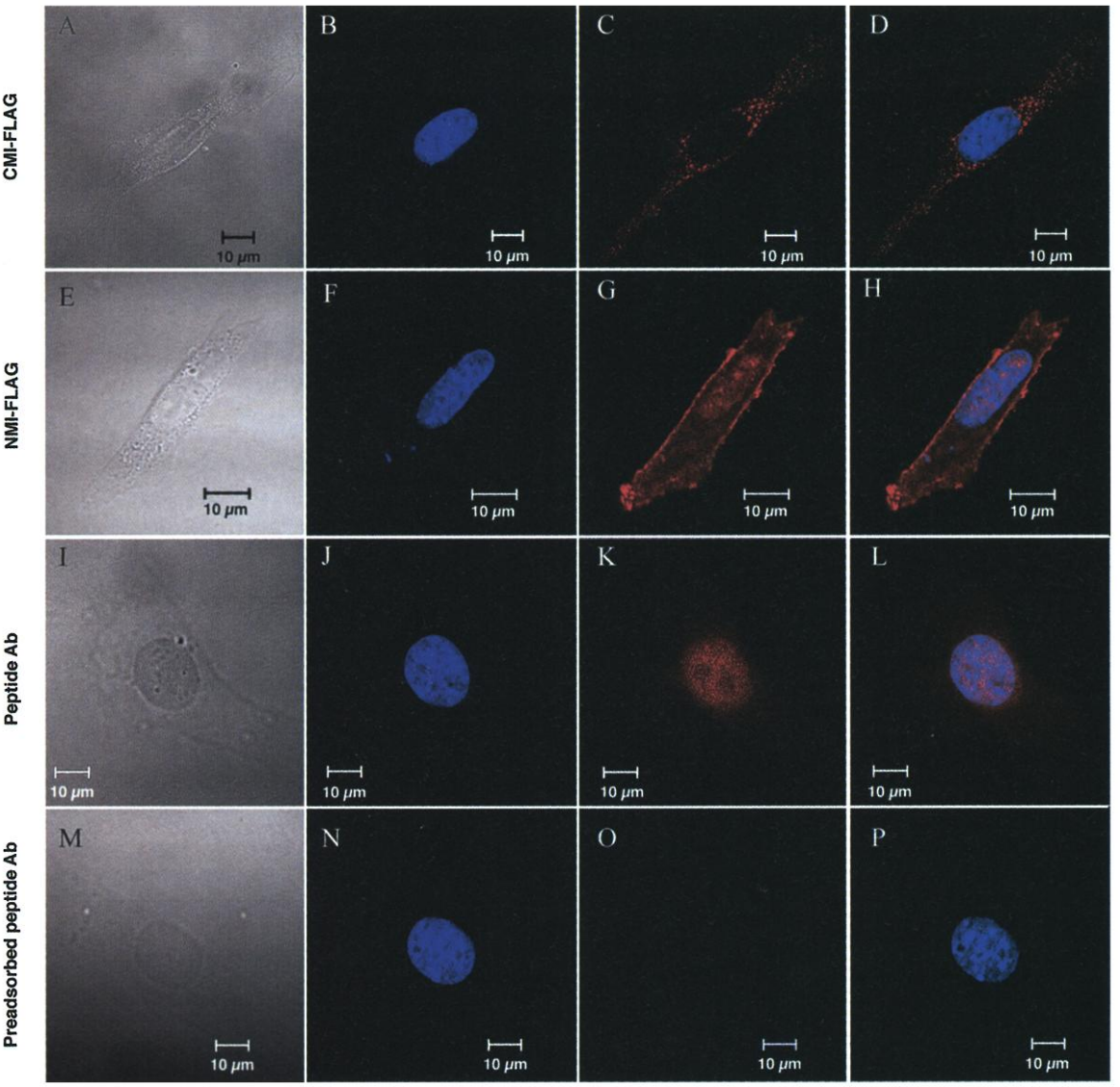

Fig. 2. Confocal images of NIH 3T3 cells. Top row: cells expressing CMIβ-FLAG; second row: cells expressing NMIβ-FLAG; third row: cells stained with affinity-purified antibody to NMIβ peptide; bottom row, cells stained with the same antibody preadsorbed with peptide. The same cell was photographed in each row. (**A**, **E**, **I**, and **M**) Differential interference contrast images. (**B**, **F**, **J**, and **N**) Cells stained with DAPI to visualize the nuclei. (**C**, **G**, **K**, and **O**) FLAG localization. (**D**, **H**, **L**, and **P**) Merged DAPI/NMIβ images. The purple color indicates the colocalization of DAPI and NMIβ. There is no nuclear staining in cells expressing CMIβ-FLAG (top row), whereas the cells expressing NMIβ-FLAG show cytoplasmic and nuclear staining (second row). The NMIβ cDNA contains start sites for NMIβ and CMIβ, and translation of the two FLAG-tagged proteins results in staining of the nucleus and the cytoplasm. The affinity-purified antibody to NMIβ peptide stains mainly the nucleus (third row); there is no staining when the antibody is preadsorbed with the peptide (bottom row).

NMIβ and RNA polymerase II (Pol II) colocalize in control cells (Fig. 4A). This colocalization was lost (Fig. 4B) when cells were treated with α-amanitin, a transcription inhibitor that stimulates the degradation of the large subunit of RNA Pol II (*18*), and decreased when cells were treated with actinomycin D (Fig. 4C), which blocks transcription by binding to DNA (*19*). Because transcriptional foci are 70 to 100 nm long (*20*), NMIβ and RNA Pol II should be within 100 nm if they are functionally related. Immunoelectron microscopy (*21*) demonstrated statistically significant numbers of NMIβ and RNA Pol II within 100 nm of each other. They were >100 nm apart in cells treated with α-amanitin or actinomycin D (Fig. 4, D to F, and Table 1).

To further investigate the interaction between NMIβ and RNA Pol II, we used antibody to NMIβ peptide to immunoprecipitate NMIβ from nuclei. Protein immunoblot analysis (*22*) showed that the large subunit of

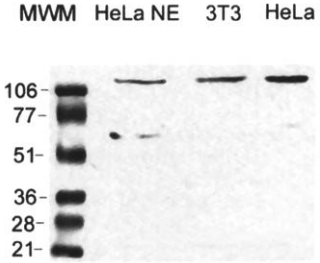

Fig. 3. Antibody to NMIβ peptide recognizes a 120-kD protein. A protein immunoblot analysis with this antibody (*16*) was performed on extracts prepared from nuclei isolated from HeLa cells (HeLa NE), NIH 3T3 cells (3T3), and HeLa cells (HeLa). The migration of marker proteins (MWM) and their molecular weight (in kilodaltons) are given. The lower band (~60 kD) is probably a degradation product of the 120-kD band.

RNA Pol II coprecipitated with NMIβ (Fig. 5A). RNA Pol II was not present in immunocomplexes when the antibody was preincubated with the peptide (Fig. 5A). In addition, antibody to NMIβ peptide inhibited RNA synthesis in vitro (Fig. 5B) (*23*). In contrast, neither the same antibody preincubated with peptide nor affinity-purified antibody to myosin II inhibited transcription (Fig. 5B).

Nuclear processes such as transcription involve large molecular complexes and require energy (*24*). The abundance of actin in the nucleus (*25*) suggests a role for myosin in the nucleus. Myosin I may be well suited as a nuclear, actin-dependent molecular motor because it does not have to form filaments to be biochemically or biologically active (*1*). Myosin I molecules contain a positively charged domain in the tail region that interacts with acidic phospholipids and powers the movement of membrane fragments on actin fila-

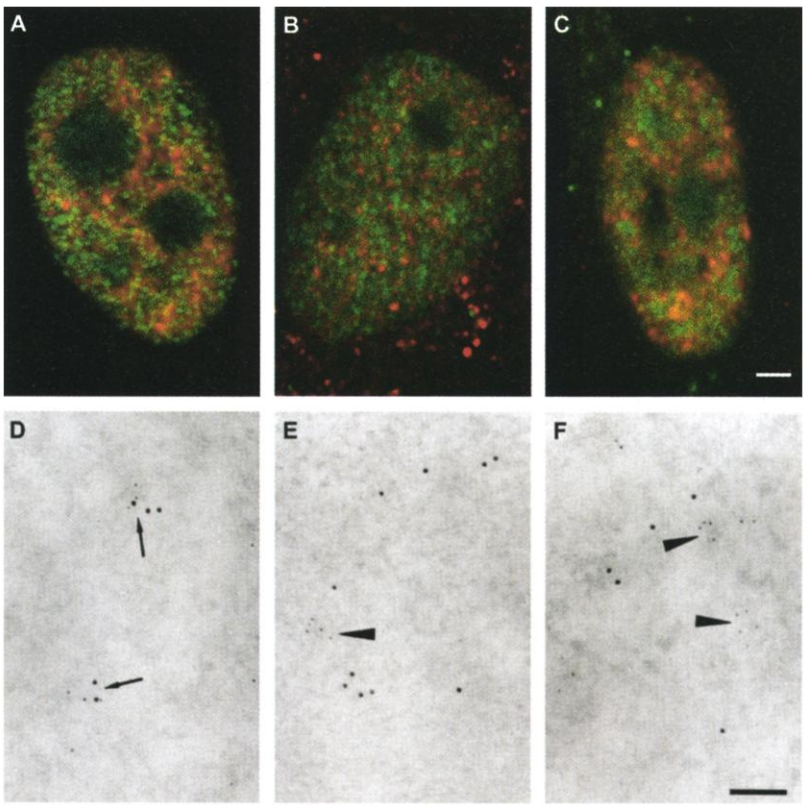

Fig. 4. Immunolocalization of NMIβ and RNA Pol II in HeLa cells. (**A** to **C**) Localization of RNA Pol II (red) and NMIβ (green) by confocal microscopy in control cells (A) and cells treated with α-amanitin (B) or with actinomycin D (C). The yellow color indicates the colocalization of RNA Pol II and NMIβ in control cells. This colocalization is practically lost (B) or reduced (C) when transcription is inhibited by α-amanitin or actinomycin D, respectively. Scale bar, 1 μm. (**D** to **F**) Double immunogold labeling of RNA Pol II (5-nm particles) and NMIβ (10-nm particles) in untreated cells (D) and cells treated with α-amanitin (E) or actinomycin D (F). Clusters of RNA Pol II are frequently intermingled with clusters of NMIβ (arrows) in control cells (D). The density of RNA Pol II labeling (arrowheads) is reduced and the colocalization is insignificant following the disruption of the Pol II complex by α-amanitin (E). The density of RNA Pol II labeling is similar to that in the control sections (arrowheads) but colocalization with NMIβ is rare following treatment with actinomycin D (F). Control samples incubated as above but minus the primary antibodies showed no significant gold labeling. Scale bar, 100 nm.

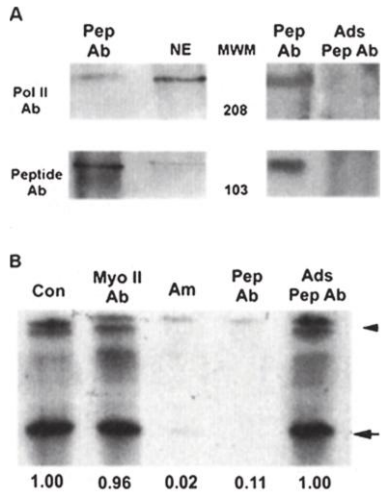

Fig. 5. Association of NMIβ and RNA Pol II. (**A**) Coimmunoprecipitation of NMIβ and RNA Pol II. NMIβ was immunoprecipitated from nuclei (*8*) using antibody to NMIβ peptide (Pep Ab) or the same antibody preadsorbed with the peptide (Ads Pep Ab) (*22*). Protein immunoblot analysis was conducted with a mAb to the large subunit of RNA Pol II (top) or with antibody to NMIβ peptide (bottom). NMIβ and RNA Pol II coimmunoprecipitated when antibody to NMIβ peptide was used, but neither was present when the immunoprecipitation was performed using preadsorbed antibody. The migration of RNA Pol II and NMIβ in a nuclear extract (NE) is shown for comparison. Molecular weight markers (MWM, in kilodaltons) are shown in the middle. (**B**) Inhibition of in vitro transcription by antibody to NMIβ peptide. HeLa cell nuclear extracts were preincubated with buffer (Con) or various agents and the transcription products analyzed (*23*). There is no transcription product in the presence of α-amanitin (Am) or antibody to NMIβ peptide. In contrast, preadsorbing this antibody with the peptide eliminated the inhibition (Ads Pep Ab), and an affinity-purified antibody to myosin II (Myo II Ab) had no effect on transcription. This experiment was repeated three to seven times; numbers at the bottom of each lane give the fractional activity relative to control, as judged by PhosphorImager quantification. The arrowhead marks the top of the gel; the arrow marks the transcription products.

ments (*1*, *5*). Similarly, NMIβ could bind to actin through the actin binding site on its head and negatively charged nuclear components through its tail region. RNA polymerases have been suggested to power the movement of DNA and transcription complexes relative to each other (*26*–*28*) in a manner analogous to energy conversion by myosin. Our data suggest that nuclear myosin I, perhaps together with RNA polymerases, could potentially power transcription.

References and Notes

1. V. Mermall, P. L. Post, M. S. Mooseker, *Science* **279**, 527 (1998).
2. T. D. Pollard and E. D. Korn, *J. Biol. Chem.* **248**, 4682 (1973).
3. M. C. Wagner, B. Barylko, J. P. Albanesi, *J. Cell Biol.* **119**, 163 (1992).
4. Y. Fukui, T. J. Lynch, H. Brzeska, E. D. Korn, *Nature* **341**, 328 (1989).
5. R. J. Adams and T. D. Pollard, *Nature* **340**, 565 (1989).
6. P. G. Gillespie, M. C. Wagner, A. J. Hudspeth, *Neuron* **11**, 581 (1993).
7. G. Nowak *et al.*, *J. Biol. Chem.* **272**, 17176 (1997).
8. Nuclei free of cytoplasmic contaminants were isolated from mouse interphase 3T3 cells as described (*7*). The nuclei (~4 × 10^7) were incubated for 5 min with diisopropyl fluorophosphate and then extracted in buffer containing deoxyribonuclease (0.5 mg/ml), ribonuclease (RNase, 0.2 mg/ml), 1 mM phenylmethylsulfonyl fluoride (PMSF), and aprotinin, leupeptin, and pepstatin (10 μg/ml each) [J. Gotzmann *et al.*, *Electrophoresis* **18**, 2645 (1997)] by passing through a 27G needle to fragment the DNA. After centrifugation, 900 μl of the supernatant was combined with 100 μl of 50 mM tris (pH 8.0), 150 mM NaCl, 1% Triton X-100, 5 mM EDTA, 1 mM PMSF, 1% SDS, and 20 μg of antibody to adrenal myosin I (*7*). The immunocomplexes were precipitated with protein A–Sepharose, separated by SDS-PAGE, and stained with Coomassie blue. The 120-kD band was excised from the stained gel and microsequenced using microcapillary high-performance liquid chromatography–electrospray ionization-tandem mass spectroscopy [J. Shabanowitz *et al.*, *Mass Spectrometry in Biology and Medicine*, A. L. Burlingame, S. A. Carr, M. A. Baldwin, Eds. (Humana, Totowa, NJ, 1999), pp. 163–177].
9. B. A. Hamilton *et al.*, *Neuron* **18**, 711 (1997).
10. F. Crozet *et al.*, *Genomics* **40**, 332 (1997).
11. C. Ruppert *et al.*, *J. Cell Sci.* **108**, 3775 (1995).
12. 5′ RACE (rapid amplification of cDNA ends) was performed using a Mouse Marathon-Ready adaptor ligated embryonic mouse cDNA library (Clontech). A primer for myosin I β (5′-CAGGAGGTAACTGAGAATGTGG-3′) that anneals 571 bp downstream from the NH_2-terminus was used with an AP-1 (adaptor primer 5′-CCATCCTAATACGACTCACTATAGGGC-3′). Polymerase chain reaction (PCR) was performed using the Advantage cDNA Polymerase mix (Clontech). DNA obtained by PCR was subjected to fluorescent nucleotide sequencing.
13. T. Hasson *et al.*, *Genomics* **36**, 431 (1996).
14. M. Kozak, *J. Cell Biol.* **108**, 229 (1989).
15. The NMIβ and CMIβ cDNAs were cloned into the pCMV-Tag4 vector (Stratagene) with the FLAG epitope at the COOH-terminal. NIH 3T3 cells growing on cover slips were transfected with 3 μg of FLAG-tagged NMIβ or CMIβ cDNA using Lipofectamine (Gibco) and cultured for 72 hours. The cells were then fixed, permeabilized (*7*), stained with a monoclonal antibody (mAb) to FLAG immunoglobulin G (Stratagene), and visualized using a Texas Red–conjugated secondary antibody. Cover slips were mounted using Vectashield with DAPI and examined using a Zeiss LSM 510 Laser confocal microscope.
16. The peptide MRYRASALGSDGVRVTGGGC (A, Ala; C,

Cys; D, Asp; G, Gly; L, Leu; M, Met; R, Arg; S, Ser; T, Thr; V, Val; Y, Tyr) was synthesized and coupled through the cysteine residue to hemocyanin, thyroglobulin, and rabbit serum albumin (RSA). Rabbits were immunized with 25 μg, each, of the peptide-hemocyanin conjugate emulsified in complete Freund's adjuvant and boosted 4 weeks later with 25 μg, each, of the peptide-thyroglobulin conjugate emulsified in incomplete Freund's adjuvant. Specific antibody to peptide was purified by applying antisera to an affinity column made by coupling the peptide-RSA conjugate to Sepharose 4B.

17. HeLa cells grown on cover slips were treated with α-amanitin (20 μg/ml for 4 hours, 40 min) or with actinomycin D (0.5 μg/ml for 1 hour). Treated and untreated cells were fixed, permeabilized, and incubated with a mAb to the large subunit of RNA Pol II (*18*) and with affinity-purified rabbit antibodies to adrenal myosin I (*7*) (both 7 μg/ml, 1 hour). The primary antibodies were visualized with Cy5-conjugated antibodies to mouse IgG and fluorescein isothiocyanate–conjugated antibodies to rabbit IgG (Jackson). Cover slips were mounted using Moviol and examined using a Leica TCS SP laser scanning confocal microscope system.
18. V. T. Nguyen *et al.*, *Nucleic Acids Res.* **24**, 2924 (1996).
19. B. Alberts *et al.*, *The Molecular Biology of the Cell* (Garland, New York, ed. 3, 1994).
20. F. J. Iborra, A. Pombo, D. A. Jackson, P. R. Cook, *J. Cell Sci.* **109**, 1427 (1996).
21. HeLa cells grown in suspension were treated with α-amanitin or actinomycin D as described (*17*). Treated and untreated cells were pelleted, fixed, and processed for immunoelectron microscopy (*7*). Sections (80 nm) were simultaneously incubated with RNA Pol II mAb (*18*) and with affinity-purified rabbit antibodies to adrenal myosin I (*7*) (both 10 μg/ml, 45 min). The primary antibodies were visualized using 5-nm gold-conjugated antibodies to mouse IgG and 10-nm gold-conjugated antibodies to rabbit IgG (British BioCell International Ltd.). The sections were contrasted with saturated uranyl acetate and examined using a Philips CM 100 electron microscope equipped with a charge-coupled device camera. A statistical analysis of colocalization was performed on 40 random digital EM images per experimental group (63.4 μm^2). Briefly, XY coordinates of all gold particles were recorded and the distances between points *x* and *y*, corresponding to pairs of 5 and 10 nm gold labels in individual images, were quantified. A histogram was generated and confidence intervals of 95% and 99% (*P* values <0.05 and 0.01, respectively) were estimated by Monte Carlo simulations of Poisson process for independent particles (A. A. Philimonenko, J. Janacek, P. Hozak, in preparation).
22. NMIβ was immunoprecipitated from isolated nuclei (*8*) using 20 μg of antibody to NMIβ peptide or 20 μg of the same antibody preadsorbed with 28 μg of peptide. The immunoprecipitates were analyzed by protein immunoblotting with antibody to NMIβ peptide or a mAb to the large subunit of RNA Pol II [S. B. Lavoie, A. L. Albert, A. Thibodeau, M. Vincent, *Biochem. Cell Biol.* **77**, 367 (1999)].
23. An in vitro transcription assay that quantifies transcription by RNA Pol II was performed using a HeLa nuclear extract system as described by the manufacturer (Promega, Madison, WI). Nuclear extract (8 units) treated with RNAguard RNase inhibitor (Pharmacia, Piscataway, NJ) was preincubated (30 min at room temperature) with buffer, 8 μg of affinity-purified antibodies to smooth muscle myosin II [P. de Lanerolle, J. R. Condit Jr., M. Tannenbaum, R. S. Adelstein, *Nature* **298**, 871 (1982)], 0.5 μg of α-amanitin, and either 8 μg of antibody to NMIβ peptide or 8 μg of the same antibody preadsorbed with 11.2 μg of peptide. HeLa template DNA (100 ng) containing the cytomegalovirus immediate early promoter was added and the reaction mixture (25 μl) was made 3 mM $MgCl_2$, 0.4 mM, each, ATP, cytidine 5′-triphosphate, and uridine 5′-triphosphate. Unlabeled guanosine 5′-triphosphate (GTP) (0.04 mM) and [α-^{32}P]GTP (10 μCi) were added and the reaction mixtures were incubated for 30 min at 30°C. The transcription products were separated by 6% acrylamide, 7 M urea denaturing gel electrophoresis, and analyzed using a PhosphorImager.
24. B. Alberts, *Cell* **92**, 291 (1998)
25. O. J. Rando, K. Zhao, G. R. Crabtree, *Trends Cell Biol.* **10**, 92 (2000).
26. H. Yin *et al.*, *Science* **270**, 1653 (1995).
27. J. Gelles and R. Landick, *Cell* **93**, 13 (1998).
28. P. R. Cook, *Science* **284**, 1790 (1999).
29. The microsequence of the 120-kD protein can be seen at *Science* Online (www.sciencemag.org/feature/data/1054436.shl).
30. We thank M. Vigneron (Illkirch, France) and M. Vincent (Quebec, Canada) for antibodies to RNA Pol II, and M. L. Chen for assistance with the confocal microscopy. Supported in part by grants from the U.S. Public Health Service to D.F.H. (NIH GM 37537) and to P. de L. (NSF MCB 9631833, NSF INT 9724168, and NIH GM 56489). P.H. is supported by the Grant Agency of the Academy of Sciences (A5039701), by the Grant Agency of the Czech Republic (304/98/1035), and by NSF (USA)/Ministry of Education of the Czech Republic grant ME 143. L.P.-D. and Y.K. were supported by an NIH Training Grant.

24 November 1999; accepted 22 August 2000

Plasma Membrane Compartmentalization in Yeast by Messenger RNA Transport and a Septin Diffusion Barrier

Peter A. Takizawa,[1] Joseph L. DeRisi,[2] James E. Wilhelm,[1] Ronald D. Vale[1,3*]

Asymmetric localization of proteins plays a key role in many cellular processes, including cell polarity and cell fate determination. Using DNA microarray analysis, we identified a plasma membrane protein-encoding mRNA (IST2) that is transported to the bud tip by an actomyosin-based process. mRNA localization created a higher concentration of *IST2* protein in the bud compared with that of the mother cell, and this asymmetry was maintained by a septin-mediated membrane diffusion barrier at the mother-bud neck. These results indicate that yeast creates distinct plasma membrane compartments, as has been described in neurons and epithelial cells.

An important means of achieving asymmetric protein distributions is through the cytoskeleton-dependent localization of cytoplasmic mRNAs (*1*). In *Saccharomyces cerevisiae*, the transcription factor Ash1p accumulates in the daughter cell nucleus, where it represses mating-type switching (*2*, *3*). The asymmetric distribution of Ash1p is created through the transport of *ASH1* mRNA to the bud tip by an actomyosin-driven mechanism (*4*, *5*). Localization of *ASH1* mRNA requires at least three proteins that are physically associated with *ASH1* mRNA: Myo4p (She1p), the myosin motor that transports *ASH1* mRNA along actin filaments to the bud tip; She3p, an adapter that mediates the association between Myo4p and *ASH1* mRNA; and She2p, which is required for the She3p-Myo4p complex to bind *ASH1* mRNA (*6*–*8*). Both She3p and Myo4p localize to the bud tip before *ASH1* mRNA expression (*9*), raising the possibility that other mRNAs are transported in yeast.

To discover other potential localized mRNAs, we identified transcripts that associate with She2p, She3p, and Myo4p using a whole-genome analysis (Fig. 1A). Each of these three proteins was immunoprecipitated from cell extracts using a Myc-epitope tag. Associated RNA was eluted and amplified by reverse transcription followed by polymerase chain reaction (RT-PCR), and the products were fluorescently labeled. An immunoprecipitate from an untagged strain served as a comparative control, and the RT-PCR product from this immunoprecipitate was labeled with a second fluorescent dye. The relative amounts of yeast mRNAs in the She protein versus control immunoprecipitations were determined by hybridization to a DNA microarray containing all *S. cerevisiae* open reading frames. *ASH1* mRNA was enriched in all three immunoprecipitates (2.9-, 2.0-, and 2.2-fold compared with control immunoprecipitates for She2p, She3p, and Myo4p, respectively), validating this approach for identifying other localized mRNAs. Other transcripts that showed a similar enrichment to *ASH1* mRNA (*10*) were then analyzed by fluorescence in situ hybridization (*5*). One of these transcripts, IST2 (increased sodium tolerance) (*11*), showed a localization pattern at the bud tip (Fig. 2A). However, in contrast to *ASH1* mRNA, which is

[1]Department of Cellular and Molecular Pharmacology and [2]Department of Biochemistry/Biophysics, and [3]Howard Hughes Medical Institute, University of California, San Francisco, CA 94143, USA.

*To whom correspondence should be addressed. E-mail: vale@phy.ucsf.edu